Bull Astr. Soc. India (2000) **28**, 15-31

Temporal behaviour of emissions from γ - ray bursts and optical/near-IR afterglows of GRB 991208 and GRB 991216

R.Sagar[1], V.Mohan[1], A.K. Pandey[1], S.B. Pandey[1] and A.J. Castro - Tirado[2]

[1] *U.P. State observatory, Manora peak, Nainital - 263 129, India*

[2] *IAA - CSIC, P.O. Box 03004, E - 18080, Granada, Spain*

Received 6 January 2000; accepted 7 February 2000

Abstract. The CCD magnitudes in Cousins R and I photometric passbands are determined for GRB 991216 and GRB 991208 afterglows respectively ~ 1 and ~ 3 day after trigger of the corresponding γ - ray bursts. Light curves of the afterglow emissions are obtained by combining the published data with the present measurements in *R* and *I* passbands for GRB 991208 and in *R*, Gunn *i* and *J* passbands for GRB 991216. They indicate that the flux decay constants of a GRB are almost the same in each passband with values ~ 2.2. for GRB 991208 and ~ 1.2 for GRB 991216 indicating very fast optical flux decay in the case of former which may be due to beaming effect. However, cause of steepening by 0.23 ± 0.06 dex in the R light curve of GRB 991216 afterglow between 2 to 2.5 day after the burst is presently not understood. Redshift determinations indicate that both GRBs are at cosmological distance with a value of 4.2 Gpc for GRB 991208 and 6.2 Gpc for GRB 991216. The observed fluence >20 kev indicates, if isotropic, release of energy ~ 1.3 X 10^{53} erg far GRB 991208 and ~ 6.7 × 10^{53} erg for GRB 991216 by these bright γ - ray flashes. The enormous amount of released energy will be reduced, if the radiation is beamed which seems to be the case for GRB 991208 afterglow. The quasi-simultaneous broad-band photometric spectral energy distributions of the afterglows are determined ~ 8.5 day and ~ 35 hour after the bursts of GRB 991208 and GRB 991216 respectively. The flux decreases exponentially with frequency. The value of spectral index in the optical-near IR region is –0.75±0.03 for GRB 991208 and –1.0±0.12 for GRB 991216.

Key words: photometry - GRB afterglow - flux decay - spectral index

1. Introduction

Gamma ray bursts (GRBs), electromagnetically the most luminous events in the Universe, are short and intense flashes of cosmic high energy (~100 keV - 1 MeV) photons. The emission from GRB afterglows, though similar in nature to the emission from supernovae, is more energetic by a few orders of magnitudes, as they release ~ 10^{51} - 10^{54} ergs or more in a few seconds. Following the naming sequence, nova and supernova, it is therefore appropriate to call GRBs as hypernova. The origin of GRBs is a mystery even after about 30 years of their accidental discovery by the Vela satellites. Interest focused on where they came from and what they were, but was hampered by lack of sufficient data to even locate them. A major break through in our understanding of GRBs has been achieved in recent years (cf. Kulkarni et al. 1999; Galama et al. 1999; Castro-Tirado et al. 1999a and references therein) mostly due to multi-wavelength observations of the long-lived emission, known as afterglow of GRB, at X-ray, optical and radio wavelengths which have become routine after launch of the Italian-Dutch X-ray satellite BeppoSAX in mid-1996, as it provides the positions of GRBs with an accuracy better than 3-5 arc minutes within hours of occurence. They indicate that most likely all GRBs are at cosmological distances.

The fireball plus blast wave is the most accepted current theoretical model for GRBs and their afterglows (see Piran 1999 for a review). The GRBs are thought to arise when a massive explosion,known as a fireball, releases a large (~$M_o c^2$) amount of kinetic energy into a volume of less than 1 light ms across. When this ultra-relativistic outflow of particles interacts with surrounding material, both forward and reverse shocks are formed. The GRB itself is thought to owe its multipeaked light curve to a series of internal shocks within a relativistic flow while the afterglows are due to the external (forward) shocks driven in the interstellar medium surrounding the burster. As the external shock interacts with increasing amount of swept-up material, it becomes less relativistic, and produces a slowly fading afterglow of X-ray, then ultra-violet, optical, infrared, millimeter and radio radiation. The afterglow emissions are most likely synchrotron radiation (Sari et al. 1998; Piran 1999 and references therein). Compared to the duration of the GRBs, afterglows in the long-wavelength bands can be long-lived. This makes now a days international multi-wavelength observing campaigns as integral part of a GRB research. The optical transient (OT) of a GRB has generally apparent R magnitude between 18 to 22, if it is detected a few hours after the burst. The 1-m class optical telescopes equipped with CCD detector are therefore capable of detecting the optical early afterglow of a GRB. As the optical follow-up observations of the GRB afterglows are valuable for understanding the nature of these bursts, we started such observations at U.P. State Observatory (UPSO), Nainital in Januray 1999 using 104-cm telescope and CCD detector under an international collaborative programme coordinated by one of us (AJCT). So far, successful photometric observations have been carried out for 3 GRB afterglows from the UPSO, Nainital. The UPSO photometric observations for GRB 990123 have been presented by Sagar et al. (1999). The same for the other two, namely GRB 991208 and GRB 991216 are presented here. These in combination with data published in GCN Observational reports are used to study flux decay and spectral index in optical and near-infrared(IR) regions. An introduction to the GRBs studied here is given below.

1.1 GRB 991208

Hurely et al. (1999) reported Ulysses, Russian Gamma Ray Experiment (KONUS) and Near Earth Asteroid Rendezvous (NEAR) detection of an extremely intense, 60 s long GRB on 1999 December 8 at 04:36:52 UT with a fluence > 25 keV of 10^{-4}erg cm^{-2} and considerable flux at > 100keV. Observations taken on 1999 December 10.92 UT with VLA at 4.86 GHz and 8.46 GHz by Frail et al. (1999) indicate presence of a compact source of spectral index of +1.4 at $\alpha_{2000} = 16^h33^m53.^s5$; $\delta_{2000} = +46^\circ27'2''$with a strong candidacy for the afterglow from GRB 991208. At the same location, optical afterglow of GRB 991208 was identified first by Castro-Tirado et al. (1999b) and confirmed by optical observations reported by Stecklum et al. (1999) and Jensen et al. (1999a). Coincident (within errors) with the location of optical and radio afterglows, Shepherd et al. (1999) detected at millimeter wavelengths the brightest afterglow of a GRB reported so far. At 15 GHz and 240 GHz, the GRB 991208 afterglows have been observed by Pooley (1999a) and Bremer et al. (1999) respectively. As this GRB seems to be unusually bright at γ - rays, optical, millimeter and radio wavelengths; its detailed study may provide new clues regarding the origin of GRB phenomena. The optical spectra of the GRB taken on 1999 December 13 and 14 with the SAO-RAS 6-m telescope (Dodonov et al. 1999b) indicate a redshift of $z = 0.7055 \pm 0.0005$, which was later also confirmed by Djorgovski et al. (1999a) with the Keck spectra take on 1999 December 14 and 15.

1.2 GRB 991216

Kippen et al. (1999) reported Burst and Transient Source Experiment (BATSE) detection of an extremely bright γ -ray burst on 1999 December 16 at 16:07:01 UT (trigger No. 7906) with total fluence above 20 keV ~ 2.6×10^{-4} erg/cm^{-2}. The event was also detected by NEAR. The burst is thus one of the brightest event detected by both BATSE and NEAR with spectral properties typical of a GRB. Its optical afterglow was detected by Uglesich et al. (1999) at $\alpha_{2000} = 05^h09^m31.^s29$; $\delta_{2000} = +11^\circ17'07''$. Coincident with this position, Taylor & Berger (1999) and Pooley (1999b) detected a radio source at 8.5 GHz and 15 GHz respectively, while Takeshima et al. (1999) discovered an X-ray afterglow. Djorgovski et al. (1999b) detected the host galaxy of the burst at z = 1.02 (Vreeswijk et al. 1999b), which extends out to ~ 1" to the west of GRB 991216 afterglow.

2. Optical observations, data reduction and calibrations

The optical observations were carried out from 1999 December 12 to 14 for the GRB 991208 afterglow and on 1999 December 17 for the GRB 991216 afterglow. We used a 2048 × 2048 pixel^2 CCD system attached at the f/13 Cassegrain focus of the 104-cm Sampurnanand telescope of the UPSO, Nainital. As GRB 991208 was located mostly in the day light sky, making optical observations was a herculean task. On all three nights, observations were obtained just before the morning twilight at large air-mass (>2) but in good photometric sky conditions. Long durations of nights at Nainital in the month of December helped us to carry out observations atleast for an hour or so on each day. One pixel of the CCD chip corresponds to 0."38, and the entire chip covers a field of ~13′×13′ on the sky. Fig. 1 shows the location of the GRB 991208 and GRB 991216 afterglows on the CCD images taken from UPSO, Nainital. For comparison, images extracted from the Digital Palomar Observatory Sky Survey (DSS) are also shown where the absence of a GRB OT is clearly seen.

Several short exposures upto a maximum of 15 minutes were generally given. In order to improve the signal-to-noise ratio of the OT, the data have been binned in 2×2 pixel^2 and also all images of a night have been stacked after correcting them for bias, non-uniformity in the pixels and Cosmic ray events. Exposure times for the stacked images of GRB 991208 afterglow in *I* were 400,1800 and 3600 s on 1999 December 12 ,13 and 14 respectively. The total exposure time for the stacked image of GRB 991216 afterglow in *R* is 85 minutes on 1999 December 17. As the OTs were generally quite faint on the stacked images, DAOPHOT profile-fitting techniques was used for the magnituted determination. On 1999 December 12 and 13 the GRB 991208 afterglow was sufficiently bright and we could derive its magnitude. However, on 1999 December 14 it had become too faint to be measured on the image. On 1999 December 13, we also observed Landolt (1992) standard stars to calibrate *I* magnitudes of the GRB 991208 afterglow. The results of UPSO observations along with other photometric measurements of GRB 991208 OT are given in Table 1.

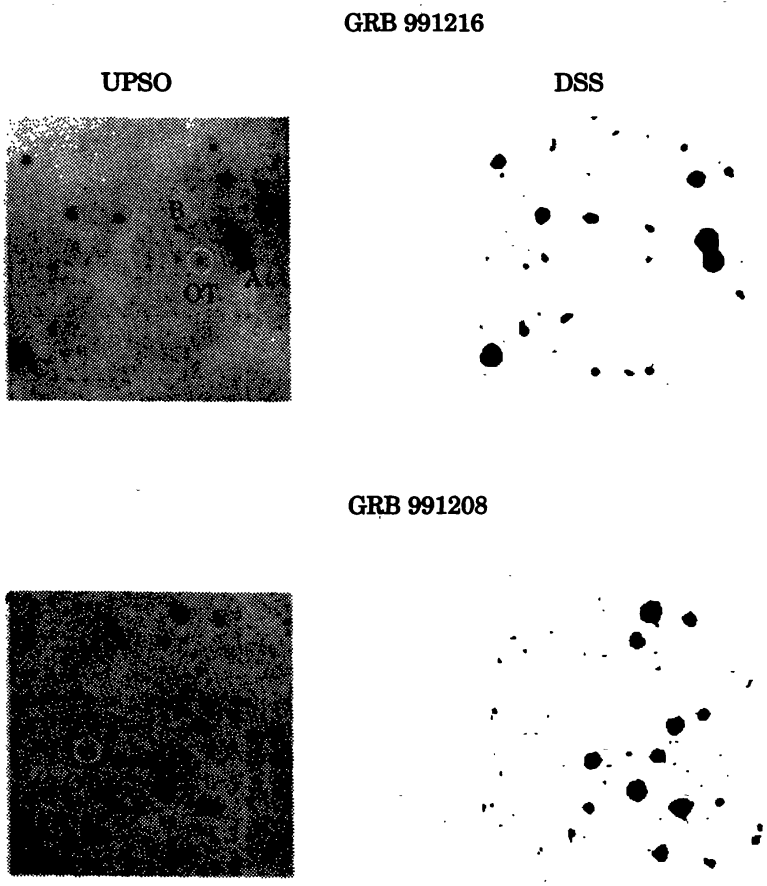

Figure 1. Finding charts are produced from the CCD images taken from UPSO, Nainital. North is top and East is left. For GRB 991208 field, the image is in *I* passband taken on 1999 December 13.0 UT while for GRB 991216, it is on 1999 Dec 17.78 UT in *R* passband. The optical transient (OT) is located inside the circle. Here only 2.′4 × 2.′4″ field of view is presented. The region corresponding to CCD image is extracted from the Digital Palomar Observatory Sky Survey and marked as DSS. A comparison of both images of the same field shows the absence of GRB afterglows on the DSS images. In the case of GRB 991208, also shown are the three comparison stars A and B (Jha et al. 1999) and C (Henden et al. 1999) calibrated by Dolan et al. (1999) in *R* band.

Table 1. Photometric observations of the GRB 991208 and GRB 991216 afterglows. Total errors in magnitude measurements are mostly ≥ 0.1 while statistical errors are always ≤ 0.1.

Time in UT	Filter	Magnitude	Source
		GRB 991208 afterglow	
Dec 99 10.27	R	18.7±0.1	Jensen et al. (1999a)
Dec 99 11.27	R	19.5±0.1	Castro-Tirado et al. (1999c)
Dec 99 11.85	R	20.0±0.2	Jensen et al. (1999a)
Dec 99 12.29	R	20.25±0.15	Masetti et al. (1999)
Dec 99 12.52	R	20.5±0.1	Granvich & Noriega-Crespo (1999)
Dec 99 13.29	R	20.3±0.2	Masetti et al. (1999)
Dec 99 13.53	R	20.92±0.06	Halpern & Helfand (1999)
Dec 99 14.14	R	21.6±0.3	Dodonov et al. (1999a)
Dec 99 14.29	R	21.25±0.15	Masetti et al. (1999)
Dec 99 15.29	R	21.6±0.3	Masetti et al. (1999)
Dec 99 11.21	I	19 to 19.5	Stecklum et al. (1999)
Dec 99 12.02	I	19.4±0.18	Present work
Dec 99 13.02	I	19.9± 0.14	Present work
Dec 99 14.00	I	> 20	Present work
Dec 99 16.68	K	19.31±0.15	Bloom et al. (1999)
		GRB 991216 afterglow	
Dec 99 17.148	R	18.63±0.02	Dolan et al. (1999)
Dec 99 17.152	R	18.64±0.02	Dolan et al. (1999)
Dec 99 17.179	R	18.73±0.05	Henden et al. (1999)
Dec 99 17.216	R	19.00±0.05	Henden et al. (1999)
Dec 99 17.293	R	19.06±0.05	Henden et al.(1999)
Dec 99 17.448	R	19.25±0.04	Dolan et al. (1999)
Dec 99 17.455	R	19.28±0.04	Dolan et al. (1999)
Dec 99 17.610	R	19.48±0.10	Jha et al. (1999)
Dec 99 17.733	R	19.89±0.13	Giveon et al. (1999)
Dec 99 17.780	R	19.70±0.08	Present work
Dec 99 18.110	R	20.12±0.10	Jensen et al. (1999b)
Dec 99 18.320	R	20.40±0.10	Jensen et al. (1999b)
Dec 99 18.320	R	20.32±0.05	Garnavich et al. (1999)
Dec 99 18.400	R	20.30±0.06	Diercks et al. (1999b)
Dec 99 18.560	R	20.57±0.05	Garnavich et al. (1999)
Dec 99 19.100	R	20.90±0.10	Jensen et al. (1999b)
Dec 99 29.410	R	23.60±0.30	Djorgovski et al. (1999b)
Jan 00 06.181	R	24.21±0.12	Schaefer (2000)
Dec 99 17.214	Gunn i	19.10±0.20	Diercks et al. (1999a)
Dec 99 17.462	Gunn i	19.90±0.20	Diercks et al. (1999a)
Dec 99 17.350	J	16.99±0.05	Garnavich et.al. (1999)
Dec 99 18.130	J	17.56±0.02	Vreeswijk et al. (1999a)
Dec 99 18.300	J	18.25±0.06	Garnavich et al. (1999)
Dec 99 18.130	H	16.74±0.02	Vreeswijk et al. (1999a)
Dec 99 18.130	K	16.76±0.02	Vreeswijk et al. (1999a)

In the field of GRB 991216, three stars (as identified in Fig. 1) are photometrically calibrated in R passband by Dolan et al. (1999) using Landoldt (1992) standard stars located in SA 93, SA 97 and SA 98 regions. The quoted uncertainty in the zero-point calibration is ± 0.03 mag. The *R* magnitudes determined by Dolan et al. (1999) agree very well with an independent measurement carried out later on by Henden et al. (2000). This indicates that Photometric calibration used in this work is secure. Present *R* magnitude is relative to comparison star A (see Fig 1). This along with other photometric measurements of GRB 991216 afterglow used in the present analysis are given in Table 1. in order to avoid errors arising due to different photometric calibrations, we have used only those *R* measurements published in GCN Observational reports whose magnitudes could be determined relative to comparison stars shown in Fig 1. In Gunn *ι* and *JHK* filters, all published photometric measurements have been used.

3. Prompt γ -ray emission

For GRB 991208, prompt γ- ray emissions were detected by KONUS and NEAR while in the case of GRB 991216, they were detected by BATSE and NEAR. We have downloaded the light curves from the archive and shown them in Figs. 2 and 3 for GRB 991208 and GRB 991216 respectively. Presence of multi-peaked spiky temporal profile in the energy distributions of both GRBs is an unambiguous indicator of a series of internal shocks within a relativistic flow. Further discussions on the γ- ray light curves of each GRB are given below.

3.1 GRB 991208

Fig. 2 shows the light curve in two energy bands accumulated by KONUS in 50 - 200 keV and by NEAR in 100 - 1000 keV. The burst profile is dominated by two strong peaks, separated by about 55 s. Almost identical temporal as well as intensity structures in the light curves at both energy bands indicate that perhaps, dominant emission is in the 100 - 200 keV range as it is common in both observed energy bands. The burst began with a strong pulse which lasted for ~ 6s. It has a sharp rise and a relatively slow decline. This is followed by a relatively weak pulse starting at ~ 40 s after the trigger. It is a relatively broad profile. Almost at the end of this pulse and ~ 52 s after trigger of the burst, the strongest pulse of this GRB started and lasted for ~ 20 s. This has almost the same rise and decline time, though the profile is multi-peaked, asymmetric and irregular. As expected, the spiky nature of the profile is clearly visible only on the 64 ms time resolution light curve. Duration (full width at half maxima) of the profile at trigger of the burst is only ~ 2s while that of the strongest one is more than 5 s. They also differ in temporal structures. The GRB is a long duration burst as it lasted for more than 70s.

3.2 GRB 991216

We show in Fig 3 the light curves of GRB 991216 in four energy bands, obtained by the BATSE on board the Compton Gamma-Ray Observatory satellite. The light curve obtained by NEAR is not shown here as it resembles to the BATSE highest energy light curve and also has poor time resolution. The burst has a complicated and irregular time profile. The event began with a weak precursor pulse lasting about 2 s, followed ~ 15 s later by an intense multi-peaked complex. The main emission lasted for ~ 17 s followed by a fainter tail that persisted for another ~ 20 s (Fig. 3).

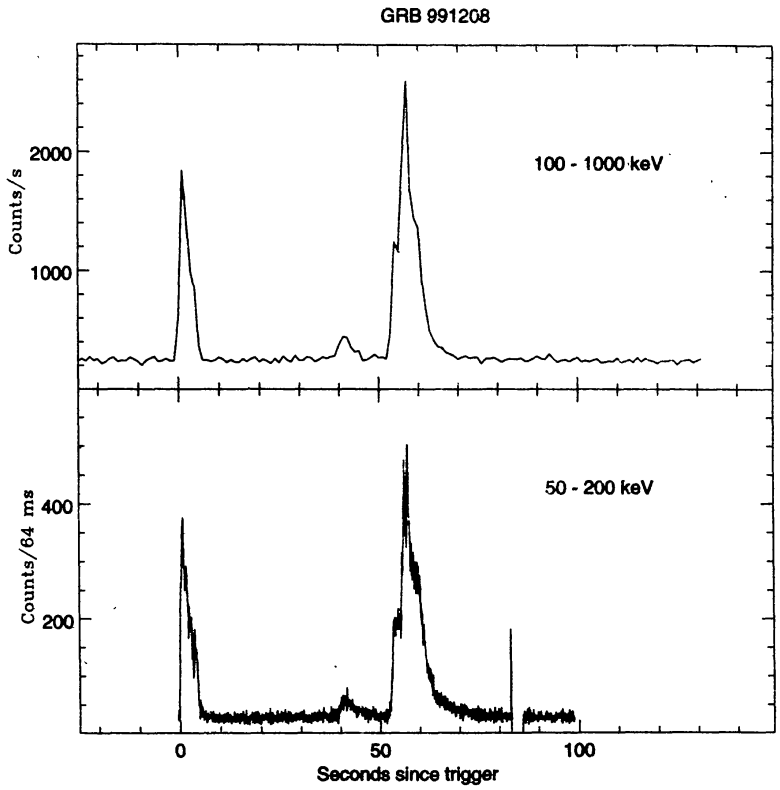

Figure 2. The NEAR and KONUS light curves of GRB 991208 in two energy ranges 50-200 keV and 100-1000 keV.

The T_{50} and T_{90} durations of the burst, as measured in the 50 - 300 keV energy range, are 6.272±0.09 s and 15.168±0.11 s respectively (Kippen 1999) indicating that it is a long duration burst. The burst lasted for ~ 60 s and it has peaks of width ~0.5 s, yielding a value of the variability index as 120.

The overall shape of the GRB 991216 in all the energy bands can be described as a fast rise starting at ~ 17 s: arrived maximum ~ 21 s and then decayed slowly. Each phase of the burst profile contains a number of well-defined short duration (full width at half-maxima generally ≤ 0.5 s) subpulse or spikes within the burst. There are 14 such spikes. We list in Table 2 their time of occurence and relative counts with respect to the first spike which has 24.3, 38.9, 49.1 and 8.5 K count/s above the background in the energy bands 20-50 keV, 50 - 100 keV, 100 - 300 keV and > 300 keV respectively. Spikes 1, 2 and 3 are during ascending phase; 4, 5 and 6 are during maxima phase and others are during descending phase of the burst. The peak of spikes occurred almost simultaneously in all the four energy bands. The variations in relative count rates of a spike from higher to lower energy bands are similar for spikes of a phase but differ from the spikes of others phases. The relative count rates are nearly the same in all energy bands for the spikes during ascending phase; they are more in > 100 keV energy range than in 20 - 100 keV range for spikes around maxima and they decrease systematically with increase in energy for spikes of descending phase. The light curves show that the low-energy emission persists longer and peaks later than high-energy emission. Particularly striking is the paucity of > 300 keV emission during the shoulder about 32 s after trigger

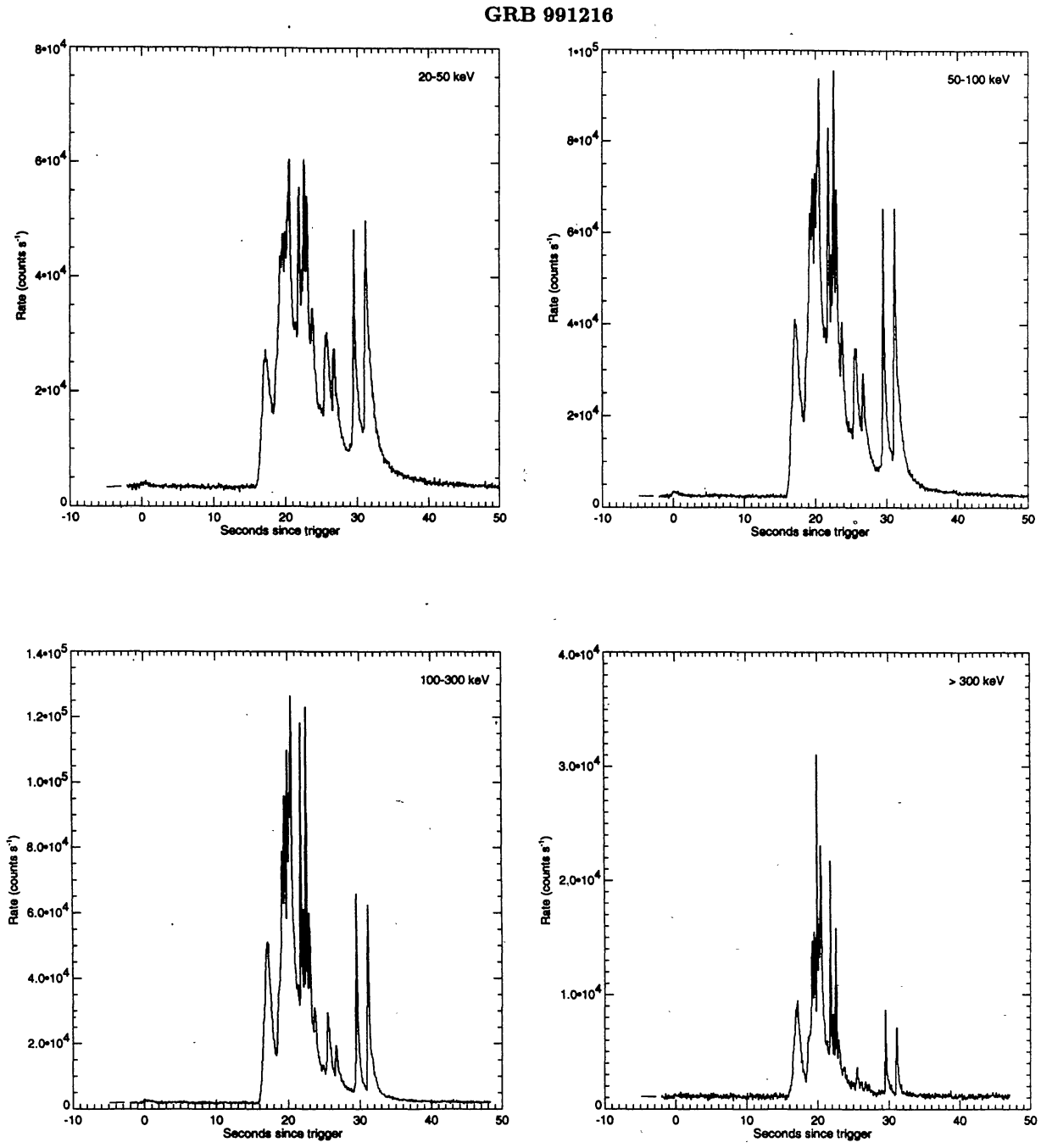

Figure 3. The BATSE light curves of GRB 991216 in four energy ranges 20 - 50 keV; 50 - 100 keV; 100 - 300 keV and > 300 keV.

of the burst. In the highest energy band emission is maximum in spike 4 and is relatively much reduced at lower energy bands. **Hard-to-soft** spectral evolution thus observed in GRB 991216 is the typical one usually (but not always) seen throught the GRB and also in sub-pulses within a burst (Fishman et al. 1999 and references there in).

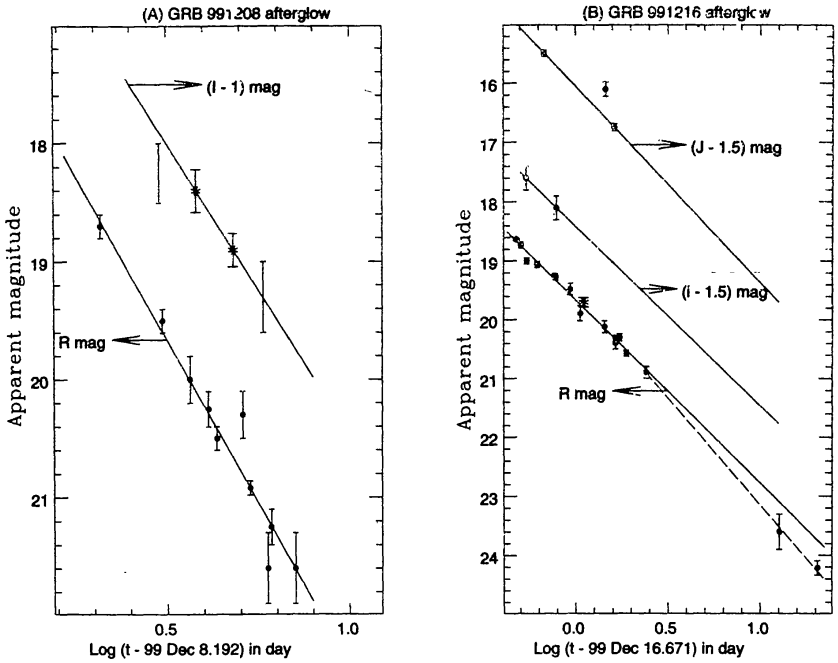

Figure 4. Light curve of (A) GRB 991208 afterglow in oprical R and I photometric passbands from 2 to 4 days after the burst while that of (B) GRB 991216 afterglow is from 1 to 20 days after trigger of the burst in *R*, Gunn *i* and *J* photometric passbands. For both GRBs, Measurements from UPSO, Nainital have been marked.

Table 2. List of well-defined γ-ray spikes during GRB 991216. Time of its occurrence (T_p)in 20 - 50 keV energy band after trigger of the burst at 1999 December 16.671 UT along with their relative count rate with respect to first spike in all the four γ-ray energy bands are given. Spikes are identified with the ascending, maxima and descending parts of the GRB 991216 burst.

Spikes	T_p (s)	Relative count rate in keV energy band 20 - 50	50 - 100	100 - 300	> 300	Phase
1	17.3	1.000	1.000	1.000	1.000	Ascendiing
2	19.3	1.693	1.591	1.554	1.611	Ascending
3	19.7	1.771	1.804	1.810	1.705	Ascending
4	19.9	1.775	1.809	2.197	3.526	Maxima
5	20.6	2.381	2.356	2.561	2.586	Maxima
6	21.9	2.216	2.089	2.368	2.452	Maxima
7	22.4	1.610	1.360	1.212	0.847	Descending
8	22.7	2.402	2.402	2.470	1.752	Descending
9	23.0	2.072	1.719	1.187	0.589	Descending
10	23.7	1.313	0.978	0.601	0.307	Descending
11	25.6	1.124	0.836	0.575	0.313	Descending
12	26.8	1.033	0.679	0.369	0.154	Descending
13	29.5	1.887	1.614	1.291	0.918	Descending
14	31.1	1.940	1.616	1.244	0.713	Descending

In the energy band 50 - 300 keV, peak flux at 64, 256 and 1024 ms intervals are 19.93±0.24, 17.80±0.11 and 14.55±0.13 μerg/cm^2/s respectively while the fluence in the BATSE energy channels 1, 2, 3 and 4 are 17.2637 ± 0.053, 22.9693 ± 0.054, 65.0656 ± 0,136 and 150.204 ± 1.167 μerg/cm^2 respectively (Kippen 1999). The hardness ratio $\frac{f100\text{-}300}{f50\text{-}100}$ is thus = 2.83 + 0.02.

4. Optical and near - IR photometric observations

Both GRB 991208 and GRB 991216 afterglow emisions have been photometred in optical and near - IR passbands and the results are published in GCN Observational reports. We have used these data in combination with the present measurements to study their flux decay and spectral index from 0.7 μm to 2.2 μm in the following sub-sections.

4.1 Light curves

In order to study the optical and near - IR photometric light curves of the GRB 991208 and GRB 991216 afterglows, we have plotted photometric measurements as a function of time in Fig. 4. The X-axis is log (t - t_o) where t is the time of observation given in Table 1 abd t_0 is the time of the trigger of GRB event which is 1999 December 8.192 UT for GRB 991208 and 1999 December 16.671 UT for GRB 991216. All times are measured in unit of day. The decay of earlier GRB afterglows appears to be well characterized by a power law $F(t) \propto (t - to)^{-\alpha}$ where $F(t)$ is the flux of the afterglow at time t and α is the decay constant. Assuming this parametric form and by fitting least square linear regressions to the observed magnitudes as function of time, we derive below the value of flux decay constant for both GRB 991208 and GRB 991216 afterglows.

4.1.1 GRB 991208

Present observations in combination with the published ones have been used to derive flux decay constants of the OT of GRB 991208. Fig. 4(a) shows the light curve in R and I photometric passbands where the useful measurements in I are only from UPSO, Nainital. The object is fading very fast, and no flattening of the light curves is observed. We obtained the following linear relations for the R and I magnitudes as function of time

$$R(t) = (16.95 \pm 0.06) + (5.47 \pm 0.09)\, log(t - t_o)$$
$$I(t) = (16.52 \pm 0.01) + (4.95 \pm 0.01)\, log(t - t_o)$$

These lines are also plotted in Fig. 4(a). In R, points which are descrepant by more than 3 σ have been excluded from the analysis. If one includes them, then the slope becomes steeper with a value of 5.92±0.55. In I, the linear relation is derived only from the UPSO observations. Other observations in I (see Table 1) are not accurate enough to be used for deriving the linear relation. Allowing for the factor - 2.5 involved in converting the flux to magnitude scale, the values of α are either 2.15 ± 0.04 or 2.37 ± 0.22 in R and ~ 2 in I passbands. This indicates that flux decays in R and I are almost similar and hence, we adopt a value of 2.2±0.1 as flux decay constant in further discussions. GRB 991208 afterglow is thus decaying much faster than afterglows of other GRBs observed so far including GRB 990123 afterglow observed earlier by us (cf. Sagar et al. 1999) where α is 1.1± 0.06. This is also the brightest afterglow detected at millimeter wavelengths to date (Shepherd et al.

1999). Thus GRB 991208 OT presents an interesting case for understanding the origin of radiation from a γ-ray burst across the entire electromagnetic band.

4.1.2 GRB 991216

In Fig. 4(B), we have plotted photometric measurements in *R*, Gunn *i* and *J* passbands as a function of time. The UPSO, Nainital measurement, identified in the figure, fits very well with the observed linear decay of the *R* magnitude. The emission from GRB 991216 OT is fading in all 3 passbands. The light curves do not exhibit flattening in any passband, though observations in *R* are until ~ 20 days after the GRB. We obtained the following linear relations for the *R*, *i* and *J* magnitudes as function of time

$$R(t) = (19.69 \pm 0.02) + (3.04 \pm 0.10)\, log\,(t - t_o)$$
$$i(t) = (19.91 \pm 0.01) + (3.05 \pm 0.01)\, log\,(t - t_o)$$
$$J(t) = (17.55 \pm 0.01) + (3.31 \pm 0.01)\, log\,(t - t_o)$$

These lines are also plotted in Fig. 4(B). In *R*, 16 points representing early observations (< 2.5 day after the burst) seem to follow a linear relation and value of the slope is derived only based on them. In *i* and *J* passbands, linear relations are derived only from the two observations provided by Diercks et al. (1999a) and Garnavich et al. (1999) respectively. The *J* magnitude of Vreewijk et al. (1999a) at 1999 December 18.13 UT lies well above the linear relation (Fig. 4(B)). By including this point in the linear fit, the slope becomes flatter with a value of 2.77 ± 0.89. Allowing for the factor -2.5 involved in converting the flux to magnitude scale, the values of α are 1.22±0.04 in R, ~ 1.22 in i and between 1.11±0.36 to 1.32 in *J* passbands. A comparison of these indicates that at early times (< 2.5 day after the burst), flux decays in optical and near - IR regions are almost similar and thus, the values of α are independent of wavelength at least in the range of 0.7 to 1.3 μ. For further discussions, we adopt a value of 1.2±0.1 for the flux decay constant of GRB 991216. This is in agreement with the early time decays of most of the GRB afterglows observed so far.

Extrapolation of the *R* linear relation derived above at the time of *R* measurements of 1999 December 29.41 UT and 2000 January 6.18 UT gives values which are brighter than the observed ones at ~ 2σ level. Somewhat steeper index is needed to fit these observations. Fitting of the least square linear regression to the last three points, shown as dotted line in the figure, yields α = 1.45 ± 0.04. This indicates a steepening of δα = 0.23 + 0.06 in the *R* light curve. More photometric observations, including those of latcr dates are required to ascertain this observed steepening in the light curve.

4.2 Spectral index of the GRB 991208 and GRB 991216 afterglows

The flux distribution of both afterglows has been determined in the wavelength range of 0.7 μm to 2.2 μm using broadband photometric measurements listed in Table 1. We used the reddening map provided by Schlegel, Finkbeiner & Davis (1998) for estimating Galactic interstellar extinction toward the bursts and found negligible for GRB 991208 but a value of $E(B - V) = 0.634$ mag for GRB 991216. In converting the magnitudes into fluxes, we have used the effective wavelengths and normalisations by Bessell (1979) for *R* and *I* and by Bessell & Brett (1988) for *J*,*H* and *K* The fluxes thus derived are accurate to ~ 10%. The Fig. 5 shows the spectrum for both GRB 991208 and GRB 991216 OTs. We fitted the observed flux distribution with a power law $F_\nu \propto \nu^\beta$, where F_ν is the flux at frequency ν and β is the spectral index. Other details are given below.

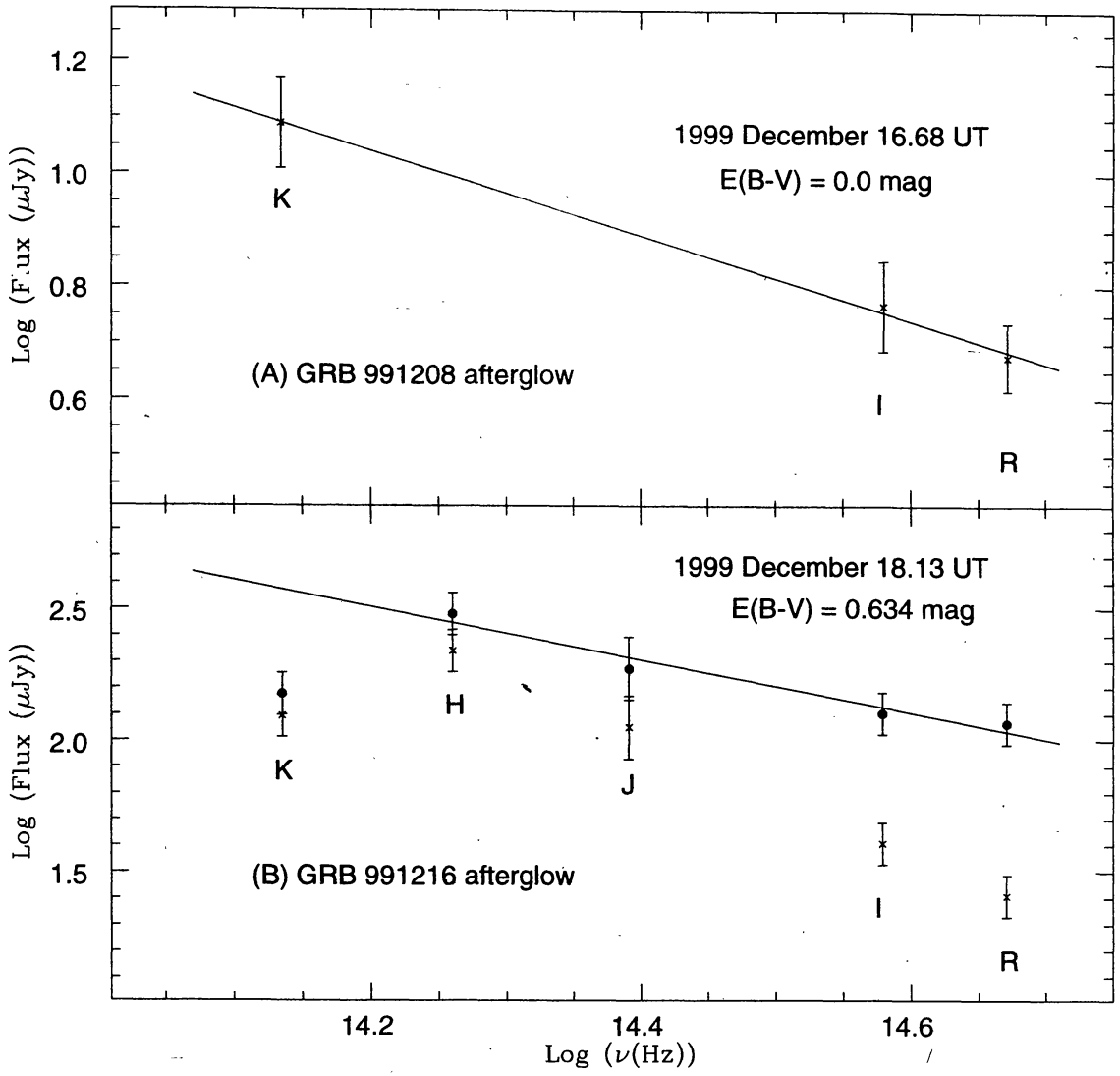

Figure 5. The spectral flux distribution of the afterglows of (A) GRB 991208 and (B) GRB 991216 at ~ 8.5 day and ~ 35 hr after the corresponding bursts. For GRB 991216 both reddened (crosses) and unreddened (filled circles) spectra are presented.

4.2.1 GRB 991208

We have constructed the GRB 991208 afterglow spectrum on 1999 December 16.68 UT. This epoch was selected for the long wavelength coverage possible at the time of observations of K magnitude. Optical flux at the wavelengths of R and I passbands has been derived using the slope of the fitted light curve shown in Fig. 4 (A) for the present epoch assuming that there is no interstellar absorption. The derived fluxes are 4.8, 5.8 and 12.3 μJy at the effective wavelengths of R, I and K passbands respectively. They are plotted in Fig. 5(A). It is observed that as the frequency decreases the flux increases with $\beta = -0.75 \pm 0.03$. This agrees very well with the value of $\beta = -0.77 \pm 0.14$ given by Bloom et al. (1999) for the spectral index between optical to IR wavelengths. A day

earlier on 1999 December 15.64, the fully calibrated Keck 10-m spectrum give the value of $\beta = -0.9 \pm 0.15$ between 0.385 to 0.885μ (Djorgovski et al. 1999a) which agrees with the optical to IR spectral index.

4.2.2 GRB 991216

We have constructed the GRB 991216 afterglow spectrum at about 35 hr after the burst, which was selected for the long wavelength coverage possible at the time of *JHK* observations (see Table 1). Using the linear equations drawn in Fig. 4(B) and the measurements listed in Table 1, we obtained for this epoch $R = 20.2$, $i = 20.4$, $J = 17.9$, $H = 16.7$ and $K = 16.8$ mag with an uncertainty of 0.2 mag. The Gunn i magnitude has been converted into Cousins I using R measurement and the relations given by Wade et al. (1979) and Besell (1979). This yields $I = 19.5 \pm 0.2$ mag. These R, I, J, H and K magnitudes have been first corrected for Galactic interstellar extinction of $E(B - V) = 0.634$ mag, which correspond to $A_{Rc} = 1.64$, $A_{Ic} = 1.24$, $A_J = 0.56$, $A_H = 0.35$ and $A_K = 0.21$ mag for the standard reddening curve given by Mathis (1990) and then converted to fluxes. The fluxes thus obtained are 115, 130, 190, 305 and 150 μ Jy at the effective wavelengths of R, I, J, H and K passbands respectively. The results are plotted in Fig. 5 (B) for both the observed and the dereddened magnitudes, in order to demonstrate the effect of Galactic extinction on the shape of the energy distribution of the afterglow. This shows that reddened spectrum becomes steeper. It is observed that as the frequency decreases the flux increases upto H passband and then it turns over. The spectrum thus may not be described by a single power law. We find that between R and H the spectral slope is -1.01 ± 0.12. By ignoring the turnover, a spectral slope of -0.45 ± 0.30 is found between R and K.

The continuum flux of the GRB 991216 afterglow determined at 1999 December 18.372 UT using J band spectrophotometry by Joyce et al, (1999) rises from ~ 150 μ Jy at 1.12 μm to ~ 220 μ Jy at 1.23 μ m, and remains approximately constant at ~ 220 μJy out to 1.33 μ m. It is thus not particularly well described by a single power law in agreement with our findings. This suggest that either not all of the near-IR flux seen is due to synchrotron emission, or a break in the synchrotron spectrum was near 1.25 μ m at the time of observation.

5. The energetics of the GRBs

Redshift determination of $z = 0.7055$ (Dodonov et al. 1999b) for the GRB 991208 afterglow and of $z = 1.02$ for the host of GRB 991216 (Djorgovski et al. 1999b), yields a minimum corresponding luminosity distances of 4.2 Gpc and 6.2 Gpc respectively for a standard Friedmann cosmological model with Hubbel constant $H_0 = 65$ km/s/Mpc, cosmological density parameter $\Omega_0 = 0.2$ and cosmological constant $\Lambda_0 = 0$(if $\Lambda_0 > 0$ then the inferred distances would increase). Considering isotropic energy emission and observed fluence above 25 keV of 10^{-4}erg/cm^2(Hurley 1999) for GRB 991208 and observed fluence > 20 keV of 255.5 μerg/cm^2 (Kippen 1999) for GRB 991216 and using the corresponding inferred luminosity distances, we estimate the γ – ray energy release to be 1.3×10^{53} erg ~ 0.07 M_0c^2 for GRB 991208 and 6.7×10^{53} erg ≈ 0.4 M_0c^2 for GRB 991216.

Of the dozen GRBs with known redshifts, five with total fluence energies > 20 keV in excess of 10^{53} erg (assuming isotropic emission) are GRB 991216 and GRB 991208 (discussed here); GRB 990510 (Harisson et al. 1999); GRB 990123 (Andersen et al. 1999; Galama et al. 1999) and GRB

971214 (Kulkarni et al. 1998). The name hypernova, coined recently, to describe such energetic events therefore seems to be most appropriate. Recent observations suggest that GRBs are associated with stellar deaths, and not with quasars or the nuclei of galaxies as some GRBs including the present GRB 991216 (see Djorgovski et al. 1999b) are found off-set from their host galaxy. However, release of huge amount of isotropic energy of ~ 10^{53} erg or more is essentially incompatible with the popular stellar death models (coalescence of neutron stars and death of massive stars). The large energy release can also not be understood with exotic models such as that of baryon decay (Perna & Loeb 1998), as the entire or a good fraction of rest mass energy of neutron stars is released in such models. There are two ways namely gravitational lensing and non-isotropic emission to reduce the enormous energy release. The possibility of the burst being amplified by gravitational lensing has been discussed at length by Kulkarni et al. (1999) in the case of GRB 990123. However, direct observational evidence for lensing lacks in GRB 990123 and others (cf. Marani et al. 1999). On the other hand, evidence for beaming seems to be present in the case of a few GRBs including GRB 991208 discussed below. Indeed, almost all energetic sources in astrophysics such as pulsars, quasars and accreting stellar black holes display jet-like geometry and hence, non-isotropic emission. Beaming reduces the estimated energy by a factor of 10 - 300, depending upon the size of its opening angle (Sari et al. 1999). The $\gamma-$ ray energy released then becomes $\leqslant 10^{52}$ erg, a value within reach of current popular models for the origin of GRBs (see Piran 1999 and references therein).

6. Discussions and conclusions

Using optical and near-IR observations (see Table 1), we obtained the values of flux decay constant and spectral index as 2.2±0.1 and -0.75± 0.03 for GRB 991208 OT and 1.2±0.1 and -1.01±0.12 for the early time flux decay of GRB 991216 afterglows. These values indicate that flux decay of the GRB 991216 is normal but that of GRB 991208 is fastest in the GRBs observed so far. The GRB 991216 OT light curve in R becomes steeper by $\delta\alpha = 0.23\pm0.06$ at late time (> 2 to 2.5 day after the burst). Before deriving any conclusion from the flux decays of these GRBs, we compare them with other well studied GRBs. Except GRB 990123 and GRB 990510, all exhibit at both early and late times a single power-law decay, generally ~ 1.2, a value reasonable for spherical expansion in the standard model. However, rapid decays and flat spectra ($\beta > -1.2$) in optical and near-IR region of the OTs of GRB 980326 with $\alpha = 1.7 \pm 0.13$ and $\beta = -0.66\pm0.7$ (Castro-Tirado & Gorosabel 1999, Sari et al. 1999); GRB 980519 with $\alpha = 2.05\pm0.04$ and $\beta = -1.05\pm 0.10$ (Halpern et al. 1999) and GRB 991208 with $\alpha = 2.2\pm0.1$ and $\beta = - 0.75\pm0.03$ (discussed here), can not be understood in terms of standard models but can either be explained by a jet (Sari et al. 1999) or by a circumstellar wind model (Chevalier & Li 1999).

Recent theoretical models on beaming of the relativistic outflow predict a break and a marked steepening in the afterglow light curve (Meszaros & Rees 1999; Rhoads 1999; Sari et al. 1999). In such models. a break in the light curve is expected when the jet makes the transition to sideways expansion after the relativistic Lorentz factor drops below the inverse of the opening angle of the initial beam. Slightly later, the jet begins a lateral expansion which causes a further steepening of the light curve. The time of occurrence of break and extent of steepening in the afterglow light curve thus depend upon the opening angle of the transient collimated outflow. At late time, when the evolution is dominated by the spreading of the jet, the value of α is expected to approach the

electron energy distribution index with values between 2.0 and 2.5 while the value of β is expected to be $-\alpha/2$, if cooling frequency has passed the observed frequency and $\frac{-(\alpha-1)}{2}$ otherwise (Sari et al. 1999). The expected values of α and β are thus in excellent agreement with the corresponding observed values of 2.4 ± 0.02 and -0.61 ± 0.12 for GRB 9901510 (Stanek et al. 1999) and 2.2 ± 0.1 and -0.75 ± 0.03 for GRB 991208 (discussed here). Fast optical flux decay and flat broadband spectrum observed in GRB 991208 here may therefore be due to effects of beaming like in GRB 990510.

Observational evidence for a break was found first in the optical light curve of GRB 990123 afterglow (Castro-Tirado et al. 1999a; Kulkarni et al. 1999) and recently in that of GRB 990510 afterglow (Stanek et al. 1999), where the light curve steepened 1.5 to 2 days after the burst. The value of $\alpha = 1.13 \pm 0.02$ for early time (3 hr to 2 day) of the GRB 990123 light curve becomes 1.75 ± 0.11 at late times (2-20 day) while the corresponding slopes for GRB 990510 are 0.76 ± 0.01 and 2.40 ± 0.02 respectively with the break time 1.57 ± 0.03 day. If the steepening observed in both cases are due to beaming, then one may conclude that it occurs within < 2 days of the burst. We therefore argue that observed steep decay in the optical light curve of GRB 991208 afterglow may be due to beaming which occurred before the start of its optical observations which is ~ 2.1 day after the burst. However, a break in the light curve of GRB afterglow can occur due to a number of causes other than beaming (Kulkarni et al. 1999; Wei & Lu 1999). We are presently unable to understand the possible cause of steepening by 0.23 ± 0.06 in the *R* light curve of GRB 991216 between 2 to 2.5 day after the burst, as beaming steepens the light curve by ~ 1 dex.

Prompt γ–ray emission light curves of both long duration bursts GRB 991208 and GRB 991216 show complicated and irregular time profile. Presence of multi-peaked and spiky temporal profile in the light curves of both GRBs is an unambiguous indicator of a series of internal shocks within a relativistic flow.

Redshift determinations yield a minimum distance of 4.2 Gpc for GRB 991208 and 6.2 Gpc for the GRB 991216, if one assumes standard Friedmann cosmology with $H_0 = 65$ km/s / Mpc. $\Omega_0 = 0.2$ and $\Lambda_0 = 0$. Both GRBs are thus at cosmological distances. Considering isotropic energy emission, we estimate enormous amount of the γ–ray energy release (1.3×10^{53} erg for GRB 991208 and 6.7×10^{53} erg for GRB 991216). These high energetics are reduced if the emission is not isotropic but collimated, as suggested by the flat spectrum and steep decay in the optical light curve of GRB 991208.

The quasi-simultaneous spectral energy distributions are determined for both GRB afterglows in optical and near-IR region. The flux decreases with frequency in both cases and follows an exponential relation with not too different spectral slopes. There are indications that the synchrotron spectrum of GRB 991216 afterglow breaks near 1.2 μm.

Acknowledgements

The authors are thankful to Prof. D. Bhattacharya for providing useful comments and suggestions. This research has made use of data obtained through the High Energy Astrophysics Science Archive Research Center Online Service, provided by the NASA/Goddard Space Flight Center.

References

Andersen M.I., et al.,1999a, Science, 283, 2075
Besell M.S., 1979, PASP 91, 589
Besell M.S., Brett J.M., 1988, PASP, 100, 1134
Bloom J.S. et al., 1999, GCN Observational Report No. 480
Bremer M. et al., 1999, GCN Observational Report No. 459
Castro-Tirado A.J., Gorosabel J., 1999, A&AS 138, 449
Castro-Tirado A.J., et al., 1999a, Science 283, 2069
Castro-Tirado A.J. et al., 1999b, GCN Observational Report No. 452
Castro-Tirado A.J. et al., 1999c, IAU Circular No. 7332
Chevalier R.A., Li Z., 1999, ApJ 520, L29
Diercks A., Ferrarese L., Bloom J.S., 1999a, GCN Observational Report No. 477
Diercks A. et al., 1999b GCN Observational Report No. 497
Djorgovski S.G., et al., 1999a, GCN Observational Report No. 481
Djorgovski S.G., et al., 1999b, GCN Observatiional Report No. 510
Dolan C., et al., 1999, GCN Observational Report No. 486
Dodonov S., et al., 1999a, GCN Observational Report No. 461
Dodonov S., et al., 1999b, GCN Observational Report No. 475
Fishman J., 1999, A&AS, 138, 395
Frail D.A., et al., 1999, GCN Observational Report No. 451
Galama T.J., et al., 1999, Nature 398, 394
Garnavich P., Noriega-Crespo A., 1999, GCN Observational Report No. 456
Garnavich P., et al., 1999, GCN Observational Report No. 495
Giveon U., Bilenko B., Ofek E., Lipkin Y., 1999, GCN Observational Report No. 499
Halpern J.P., et al., 1999, ApJ 517, L105
Halpern J.P., Helfand D.J., 1999, GCN Observational Report No. 458
Harrison F.A., et al., 1999, ApJ 523, L121
Henden A. et al., 1999, GCN Observational Report No. 473
Henden A., Guetter H., Vrba F., 2000, GCN Observational Report No. 518
Hurley K., et al., 1999, GCN Observational Report No. 450
Jensen B.L., et al., 1999a, GCN Observational Report No. 454
Jensen B.L., et al., 1999b, GCN Observational Report No. 498
Jha S., et al., 1999, GCN Observational Report No. 476
Joyce D., Rhoads J., Ali B., Dell'Antonio I., Jannuzi B., 1999, GCN Observational Report No.511
Kippen R.M., 1999, GCN Observational Report No. 504
Kippen R.M., Preece R.D., Giblin T., 1999, GCN Observational Report No. 463
Kulkarni S.R. et al., 1999, Nature 398, 389
Kulkarni S.R. et al., 1998, Nature 393, 35
Landolt A.U., 1992, AJ 104, 340
Marani G.F., et al., 1999, ApJ, 512, L13
Masetti N. et al., 1999, GCN Observational Report No. 462
Mathis J.S., 1990, ARAA, 28, 37
Mészáros P., Rees M.J., 1999, MNRAS, 306, L39
Perna R., Loeb A., 1998, ApJ, 509, L85
Piran T., 1999, Physics Report, 314, 575
Pooley G., 1999a, GCN Observational Report No. 457
Pooley G., 1999b, GCN Observational Report No. 489
Rhoads J.E., 1999, ApJ, 525, 737
Sagar R., Pandey A.K., Mohan V., Yadav R.K.S., Nilakshi, Bhattacharya D., Castro-Tirado A.J., 1999, BASI, 27, 3
Sari R., Piran T., Halpern J.P., 1999, ApJ, 519, L17
Sari R., Piran T., Narayan R., 1998, ApJ, 497, L17
Schaefer B., 2000, GCN Observational Report No. 517
Schlegel D.J., Finkbeiner D.P., Davis M., 1998, ApJ, 500, 525

Shepherd S. et al., 1999, GCN Observational Report No. 455
Stanek K.Z., et al., 1999, ApJ, 522, L39
Steeklum B. et al., 1999, GCN Observational Report No. 453
Takeshima T., Markwardt C., Marshall F., Giblin T., Kippin R.M., 1999, GCN Observational Report No. 478
Taylor G.B., Berger E., 1999, GCN Observational Report No. 483
Uglesich R., Mirabal N., Halpern J., Kassin S., Novati S., 1999, GCN Observational Report No. 472
Vreeswijk P.M. et al., 1999a, GCN Observational Report No. 492
Vreeswijk P.M. et al., 1999b, GCN Observational Report No. 496
Wade R.A., Hoessel J.G., Elias J.H., Huchra J.P., 1979, PASP 91, 35
Wei D.M., Lu T., 1999, preprint astr-ph/9908273